Simulation of polar stratospheric clouds: 1. Microphysical characteristics

Ya.A. Virolainen, Yu.M. Timofeyev, A.V. Polyakov, H. Steele,* K. Drdla, and M. Newchurch*****

Scientific Research Institute of Physics at St. Petersburg State University, Russia
** State University of California, Northridge, USA*
*** NASA, USA*
**** University of Alabama, Huntsville, USA*

Received July 26, 2004

Microphysical properties of stratospheric aerosol and polar stratospheric clouds (PSCs) are simulated based on the up-to-date numerical model of formation and transformation of aerosol particles. Overall, the analyzed ensemble totals 255949 realizations and may be considered as a broad representative ensemble of stratospheric aerosol states and PSC under polar and midlatitude winter conditions of the northern hemisphere (45–90°N). The means and covariance matrices of the size distribution function (SDF) for different scenarios of PSC transformation are constructed. Possibilities of optimally parameterization of SDF and its higher-order moments are explored. It is shown that, to describe all SDF realizations with the error no larger than 5–10%, it is sufficient to use just 6 expansion coefficients, rather than specifying SDF *a priori* in 39 bins. Use of "foreign" vectors as a basis in parameterizations by use of other models insignificantly changes the relative errors of SDF parameterization.

Introduction

Polar stratospheric clouds (PSCs) form at altitudes from 14 to 29 km at extremely low temperatures, episodically observed under conditions of polar winters in the stratosphere, during simultaneous condensation of water vapor and nitric acid on sulfate particles of background stratospheric aerosol, as well in separate cases during particle freezing.[1] Recently it has been found that PSCs play a significant role in stratospheric chemistry, actively participating in destruction of the ozone layer.[2,3]

In recent years, some results have been obtained in the studies of microphysical and optical properties of PSCs using both *in situ* and remote measurements. For instance, the satellite experiments with ILAS, POEM, and SAGE instrumentation studied the spectral extinction coefficients of PSCs and attempted to solve the inverse problem of retrieval of size distribution function (SDF) of PSC particles.[4–7] Correct solution of this inverse problem requires specification of *a priori* information on SDF, especially considering that the measurements of spectral extinction coefficient of PSC particles have poor information content on the SDF. On the other hand, the *in situ* measurements of PSC SDF are still sparse, so the PSC statistical characteristics and optical properties cannot be constructed (both in terms of the corresponding SDF covariance matrices and matrices of extinction coefficient) based on the empirical data.

Another way of constructing such covariance matrices is based on numerical simulation of SDFs or aerosol optical properties.[8–10]

In this paper, a detailed model of PSC formation and decay is used to generate a large ensemble of SDF realizations and to study the statistical properties of SDF of PSC particles. In the subsequent publication,[11] we study the statistical properties of spectral extinction coefficient of PSC particles [hereinafter, aerosol extinction coefficient (AEC)] and capabilities of regression approach to solution of inverse problem of retrieval of SDF of PSC particles from AEC measurements.

1. Simulation of the stratospheric aerosol state

The microphysical PSC model was developed to simulate the formation, growth, and evaporation of particles along air trajectories in the Arctic stratosphere.[12] This model consists of three main blocks operating jointly, namely, modules of aerosol microphysics, heterogeneous chemistry, and photochemistry. For Arctic winter of 1999/2000, we calculated a large number of long-term trajectories; these were based on the data of United Kingdom Meteorological Office and allowed us to construct a three-dimensional pattern of the evolution of the Arctic vortex. The simulation spanned time period from November 1, 1999 until April 15, 2000. All trajectories were initiated and we constructed initial

0235-6880/05/03 243-05 $02.00 © 2005 Institute of Atmospheric Optics

profiles of NO_y (based on N_2O measurements), H_2O, and H_2SO_4 (based on measurements and climatically mean data).

To construct PSC ensembles, we used several scenarios differing by the set of assumptions on microphysical parameters and processes governing the PSC formation and transformation. For this we calculated the evolution of SDFs for particles of different types potentially present in PSCs, namely: (1) Liquid Aerosol, liquid sulfate particles (two- or three-component solutions, depending on temperature); (2) SAT aerosol, frozen particles of sulfur acid tetrahydrate; (3) NAT PSC, solid particles of nitrous acid tetrahydrate, as well as (4) water ice PSC, frozen water particles. The PSC simulation results were carefully compared with the data of SOLVE measurement campaign,[13] as well as of earlier campaigns[14,15] (see Ref. 13 for a more detail). The authors of the PSC development models indicated that only four of the considered models [Het0many.sed (I), Het16many.sed (II), Met_1_m10.once.sed (III), and Nadhet1many.sed (IV)] well agree with experimental data; therefore in the below discussion we will separately consider only these models, using the corresponding digital notation for particle ensembles. To describe the microphysical properties and the corresponding optical characteristics (AEC, see Ref. 11), we will consider the statistical properties of both individual PSC types and total PSC ensemble (SUM). In addition, since the numerical model[13] reproduces not only PSCs but also entirely all states of stratospheric aerosol, we tried to collect in one ensemble and analyze the realizations pertaining only to PSCs. For this we used a criterion characterizing AEC at the wavelength of 1 μm and, in addition to the total ensemble SUM, we constructed subensemble SUM1, from which we excluded realizations of AEC less than 10^{-3} km^{-1}. It should be noted that all realizations in the SUM1 ensemble pertain deliberately to PSCs, that is the aerosol state considerably exceeds characteristic mean background stratospheric values. The number of realizations in SUM1 ensemble is 33.7% of the total number of realizations.

2. Microphysical PSC characteristics

Each realization of the PSC state is described by its SDF in the interval of radii 0.01–63 μm (total number of intervals is 39, with the step of 0.23 of the logarithm of radius). Total number of PSC realizations in the total ensemble is 255 949. For each ensemble separately we calculated SDF covariance matrices $n(r)$, as well as SDF functionals: total number of particles N and the area S and volume V of all aerosol particles according to the formulas:

$$N = \int_0^\infty n(r)\mathrm{d}r; \quad S = \int_0^\infty \pi r^2 n(r)\mathrm{d}r;$$

$$V = \frac{4}{3}\int_0^\infty \pi r^3 n(r)\mathrm{d}r. \qquad (1)$$

Let us consider the average SDF values for particles in each fraction for different PSC models. Figure 1 shows these values for PSC scenarios I–IV. It is seen that SDF of aerosol particles (Liquid and SAT) has maximum at sizes as small as decimal fractions of micron, whereas PSC particles (NAT and Water Ice) peak at radii of several microns or even tens of microns.

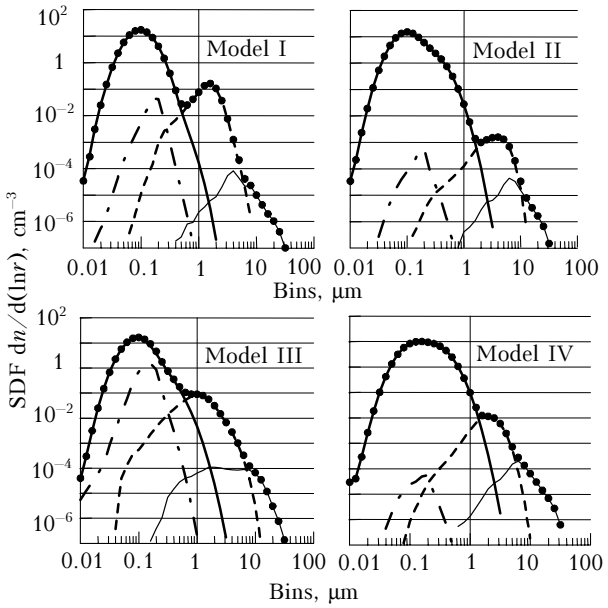

Fig. 1. Mean values of the size distribution function in all fractions for PSC models I–IV: (——) Liquid aerosol; (—·—) SAT aerosol; (– – –) NAT PSC; (——) Water Ice PSC; (•) all particles.

At the same time, the number of particles in the bins is typically maximum (11–16 cm^{-3}) for Liquid aerosol, and these same particles also determine the shape of the total SDF for particles smaller than 1 μm in size. Although the number of SAT particles for ensemble III is relatively large (up to 2 cm^{-3}), because of coincidence of SDF maxima SAT particles largely "obscure" the particles in Liquid fraction. In ensembles I and III, the maximum (up to 0.1–0.2 cm^{-3}) is observed for NAT particles. A distinct feature of the model I is the most narrow SDF in the region of maximum, while that of the model IV is the most wide SDF and somewhat skewed toward large-size particles. Thus, depending on particle size, the main contribution to SDF comes from Liquid (partially SAT) fraction for particles with radii from 0.01 to 1–2 μm, from NAT and Water Ice fractions for size range 1–10 μm, and from Water Ice fraction at radii greater than 10 μm.

We note that the root-mean-square (rms) variations of SDF in the region of maximum reach 40–80%, depending on considered scenario; at the same

time, in SUM1 ensemble for particles larger than 0.2 μm the SDF variations are somewhat stronger than in the SUM ensemble. Analysis of the SDF mean values has shown that in SUM1 ensemble, compared with the SUM one, a redistribution of particles over size range takes place. For instance, around the SDF peak the particles are somewhat depleted in number (15 versus 16 cm^{-3}), while in the region of aerosol particle radii 0.15–0.5 μm the number of particles increases (several times, from 1 to 3–4 cm^{-3} for radii on the order of 0.3–0.4 μm). Supposedly, for aerosol realizations with large AEC, a significant role is played by large particles of Liquid Aerosol fraction.

Such an information on contributions of different fractions to the total integral characteristics (different SDF moments), namely to the total particle concentration N and to total area S and total volume V for the total PSC ensemble is presented in the Table. The bottom line of the Table shows the ensemble mean effective particle radius r_{eff}, defined as the ratio of V to S times 3/4, for particles of each fraction and for all particles. Given in parentheses is the percentage of realizations with a given fraction in total number of realizations of the ensemble. As seen, the smallest effective radius (0.12 μm) is observed for particles of SAT fraction, and the largest effective radius (15.45 μm) for Water Ice fraction, whose particles are present in only 3.5% of realizations. Effective particle radius, averaged over total ensemble, is 0.8 μm. Also shown in the Table are relative rms deviations of considered parameters from the relevant mean values. From analysis of the Table we can conclude that in the total ensemble of PSC realizations the Liquid particles contribute 97.7% to the total number of particles and 64.2% (33.5% for NAT) to the total particle area. Contribution to the total volume is 74.2% for NAT (18% for Liquid, and 7.7% for Water Ice) particles. For the SUM1 ensemble, the contribution of particles in different fractions to N is approximately the same as for SUM, while the contribution of particles in the NAT fraction to the total area is somewhat larger (40%). In ensembles of PSC realizations I–IV, the mean N value is almost totally determined by Liquid fraction, while the contribution of other particles to this characteristic does not exceeds 6%. At the same time, for the total particle area in scenarios I and III, the contribution of these particles is of the same order as the contribution coming from NAT particles. For these models (and, correspondingly, for SUM ensemble), the NAT fraction has 1–2 orders of magnitude larger contribution to total particle volume than that of Liquid fraction.

From analysis of variations of SDF moments for different fractions it can be concluded that the total number N of particles changes insignificantly (rms deviation from the mean is 28–41%). This is because N is primarily determined by fine particles, i.e., Liquid Aerosol fraction, representing background stratospheric aerosol, always present in some amount in the atmosphere, and not determining directly PSC parameters. At the same time, the rms variations of the number of Water Ice particles ranges from 2 000 to 6 000%, although their mean number is insignificant in comparison with other fractions. The strongest variations are also observed for other SDF moments of this fraction. From a comparison of different scenarios we can conclude that the model IV exhibits the strongest variations of SDF moments of SAT particles (1 500–2 000%), while for other scenarios these variations are an order of magnitude lower. It is also worth noting that the variations of SDF moments in the SUM1 ensemble are weaker than in the SUM ensemble. For instance, the rms variations of the three first SDF moments are, respectively, 38, 85, and 174% for the total ensemble, and 32, 55, and 125% for the SUM1 ensemble.

3. Optimal parameterization of SDF of aerosol particles and integral SDF parameters

To construct a SDF parameterization with respect to aerosol particle radii, we used an optimal parameterization based on SDF decomposition over basis composed of eigenvectors of SDF covariance matrices:

$$y(x_i) = \bar{y}(x_i) + \sum_{p=1,n} a_p f_p(x_i). \qquad (2)$$

Here, $f_p(x_i)$ are the eigenvectors of covariance matrix D of SDF of the ensemble considered ($Df = \lambda f$, λ is the eigenvalue); a_p are the corresponding expansion coefficients; $y(x_i)$ are the SDF values for particles of radius x_i; and $\bar{y}(x_i)$ are the average SDF values.

Means $\bar{x}$ and variations σ (%) of SDF moments of different aerosol fractions in total PSC model (255 949 model realizations)

Fraction	Liquid aerosol		SAT aerosol		NAT PSC		Water Ice PSC		All particles	
Parameter	$\bar{x}$	σ	$\bar{x}$	σ	$\bar{x}$	σ	$\bar{x}$	σ	$\bar{x}$	σ
N, cm^{-3}	18.42	38	34.3	250	0.87	152	0.0001	4006	18.85	38
S, $\mu m^2 \cdot cm^{-3}$	1.15	117	0.03	217	0.6	128	0.01	2088	1.8	85
V, $\mu m^3 \cdot cm^{-3}$	0.40	229	0.006	208	1.64	118	0.17	1891	2.2	174
r_{eff}, μm	0.17 (100%)		0.12 (95.5%)		2.78 (99.9%)		15.45 (3.5%)		0.8	

This parameterization was performed for all considered PSC ensembles. Figure 2 shows first four (*1–4*) eigenvectors of matrix D for four scenarios of the PSC development. From Fig. 2 it is seen that the behavior of the first and second eigenvectors differs for different scenarios. For instance, in models II and IV the second eigenvector assumes only positive values in particle size range 0.07–0.6 μm, while the first eigenvector takes zero value in the region of 0.2 μm. On the contrary, for models I and III the second eigenvector takes zero value in the region of 0.1 μm, while the first is positive in the particle size range 0.03–0.2 μm. In addition, in scenario I the fourth eigenvector slightly increases in the size range 1.5–2.5 μm due to the influence of PSC particles of NAT fraction (see Fig. 1). Also, it should be noted that eigenvectors of SUM1 ensemble are close to vectors of the ensemble II.

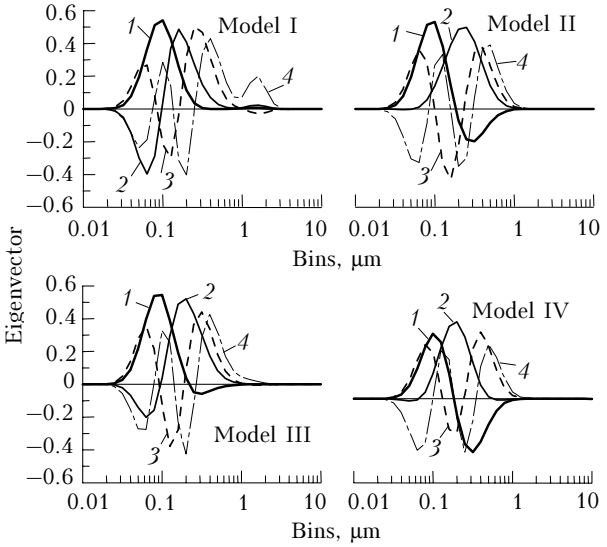

Fig. 2. Eigenvectors of SDF covariance matrix of aerosol particles of all fractions, calculated for PSC ensembles I–IV.

Analysis of first seven eigenvalues of the SDF covariance matrices for different models has shown that ensemble I differs from all other ensembles in that its eigenvalues faster decrease with growing vector number. Already sixth eigenvalue is more than two orders of magnitude less than the first value. At the same time, for ensemble III, even seventh eigenvalue is less than the first value by less than two orders of magnitude; therefore, in this case one should not expect high accuracy of parameterization for small number of eigenvectors. At the same time, overall, using eigenvalue analysis and limiting oneself to two orders of magnitude of the drop of higher-order eigenvalues relative to the first value, in most situations just first six eigenvalues can safely be retained in decomposition. The ratio of sixth to first eigenvalue is 0.016 for SUM ensemble and 0.015 for SUM1 ensemble.

Figure 3 shows the absolute rms error of SDF parameterization (2) of aerosol particles for all considered PSC models, as well as SUM ensemble, versus retained number of vectors. As expected, for small number of eigenvectors (less than 5) the approximation error is the least for model I, and for larger number of vectors it is the least for models II and IV. For model III and aggregate model the parameterization accuracy is lower than in other models.

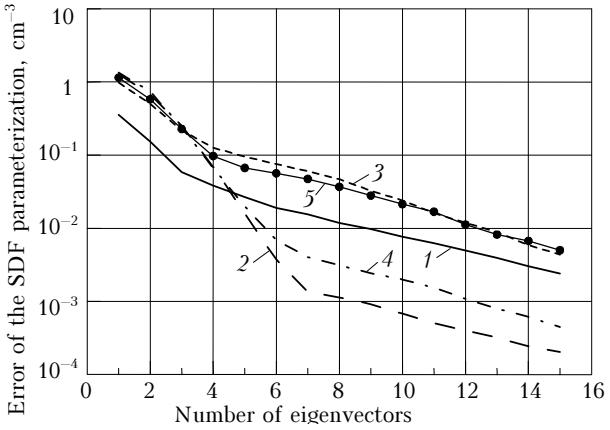

Fig. 3. Dependence of absolute error of optimal SDF parameterization on particle size for different numbers of retained vectors for different PSC ensembles: (*1*) model I; (*2*) model II; (*3*) model III; (*4*) model IV; and (*5*) SUM.

Analysis of behavior of approximation error as a function of aerosol particle size has shown that, over the range of particle sizes for which SDF value is no more than two orders of magnitude lower than the maximum value, 4–6 vectors in decomposition (2) will be sufficient to restrict the error of optimal parameterization to 1%. An exception is model III, which under these conditions yields 5–8% error of size parameterization.

For particle size range 0.04–0.3 μm, with the use of 5–6 vectors in approximation of the SUM ensemble, the parameterization is accurate to within 2–3%. In SUM1 ensemble, the accuracy of approximation in the particle size range from 0.2 to 3 μm is somewhat higher than in the total ensemble. For instance, the parameterization error of less than 10% is observed in the size range from 0.02 to 0.55 μm for the SUM1 ensemble, and only in the region of particles less than 0.45 μm in size for the total ensemble.

Dependence of the relative error of optimal SDF parameterization on particle size for PSC ensembles I–IV and SUM with the use of first six eigenvectors in Eq. (2) is shown in Fig. 4.

It can be seen that in the region of SDF maximum, the errors for all models do not exceed 5–10%. At the same time, for scenario II the relative error in the region of SDF maximum does not exceed 1%. We would like to note that SDF parameterization errors substantially increase both for very small particles, and for particles with radii larger than 1 μm. Also, we performed calculations in which we used as a basis the vectors for the given

models, while parameterization over this basis was carried out for some other models, that is for parameterization we used "foreign" vectors. Such estimates are important because ensembles of PSC realizations are treated with different models; and this is usually done without confident information about precisely what model must be used in a given specific case of real data analysis. Therefore, it is important to estimate the error the SDF parameterizations introduced due to wrong use of "foreign" vectors in the SDF parameterization. The calculations have shown that the use of "foreign" vectors as a basis in parameterization using other models insignificantly changes the relative errors of the SDF parameterization.

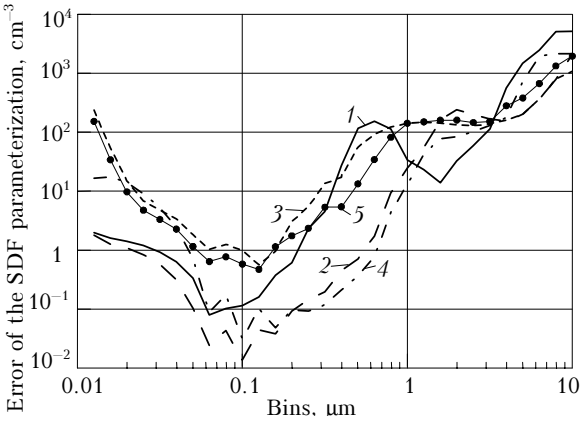

Fig. 4. Dependence of relative error of optimal SDF parameterization on the particle radius with the use of six eigenvectors of SDF covariance matrix in decomposition for different PSC ensembles: (*1*) model I; (*2*) model II; (*3*) model III; (*4*) model IV; and (*5*) SUM.

In addition to uncertainties of SDF parameterization itself, we also analyzed the errors of calculation of integral SDF characteristics, performed with the use of parameterization. In this analysis, quite high accuracy was obtained only for the total number of particles. For instance, for all considered ensembles, already with first three eigenvectors used in the calculation the error of N parameterization did not exceed 1%. For the total particle area, use of just six eigenvectors may reduce uncertainty about natural variations of the area by the factor of 2 (7) for the model III (II). The uncertainty of total particle volume decreases by no more than 10–20%. This is because the higher-order SDF moments are determined by larger particles for which the relative error of SDF parameterization is very high, and in these cases it is impossible to significantly reduce the *a priori* uncertainty.

Conclusion

Microphysical properties of stratospheric aerosol and PSCs have been modeled using modern numerical model of aerosol particle formation and transformation.[12] The SDF mean values and covariance matrices are constructed for different scenarios of PSC development. Optimal parameterization of SDF and its statistical moments, using optimal empirical basis, is evaluated. It is shown that, to describe all SDF realizations with the error not exceeding 5–10%, it is sufficient to use just 6 expansion coefficients, rather than specifying SDF in 39 bins. Use of "foreign" vectors as a basis in parameterization by use of other models insignificantly changes the relative errors of the SDF parameterization.

Acknowledgments

This work is supported by St. Petersburg Administration (Grant PD03-1.5-114), National Aeronautics and Space Administration (Grant NAG 5–11248), Russian Foundation for Basic Research (Grant 03-05-64626), Universities of Russia (Grant UR.01.01.044).

References

1. J.H. Seinfeld and S.N. Pandis, *Atmospheric Chemistry and Physics. From Air Pollution to Climate Change* (John Wiley & Sons, Inc., New York–Chichester–Weinheim–Brisbane– Singapore–Toronto, 1998), 1326 pp.
2. S. Solomon, R.R. Garcia, F.S. Rowland, and D.J. Wuebbles, Nature **321**, No. 3, 755–758 (1986).
3. *WMO. Scientific Assessment of Ozone Depletion 1994.* WMO Report 37 (Geneva, 1995).
4. M.D. Fromm, J.D. Lumpe, R.M. Bevilacqua, E.P. Shettle, J.S. Hornstein, S.T. Massie, and K.H. Fricke, J. Geophys. Res. D **102**, No. 19, 23659–23672 (1997).
5. H.M. Steele, K. Drdla, R.P. Turco, J.D. Lumpe, R.M. Bevilacqua, Geophys. Res. Lett. **26**, No. 3, 287–290 (1999).
6. K.-M. Lee, J.H. Park, Y. Kim, W. Choi, H.K. Cho, S.T. Massie, Y. Sasano, and T. Yokota, J. Geophys. Res. D **108**, No. 7, 4228 (2003).
7. G.E. Neduluha, R.M. Bevilacqua, M.D. Fromm, K.W. Hoppel, and D.R. Allen, Geophys. Res. Lett. **30**, No. 15, 1796 (2003).
8. A.V. Polyakov, A.V. Vasiliev, and Yu.M. Timofeyev, Izv. Ros. Akad. Nauk, Ser. Fiz. Atmos. Okeana **37**, No. 5, 646–657 (2001).
9. Yu.M. Timofeyev, A.V. Polyakov, H.M. Steele, and M.J. Newchurch, Appl. Opt. **42**, No. 12, 2635–2646 (2003).
10. Ya.A. Virolainen, A.V. Polyakov, and Yu.M. Timofeyev, Izv. Ros. Akad. Nauk, Ser. Fiz. Atmos. Okeana **40**, No. 2, 255–266 (2004).
11. Ya.A. Virolainen, Yu.M. Timofeyev, A.V. Polyakov, H. Steele, K. Drdla, and M. Newchurch, Atmos. Oceanic Opt. (in print).
12. K. Drdla, "Applications of a model of polar stratospheric clouds and heterogeneous chemistry," Ph. D. thesis, UCLA (1996).
13. K. Drdla, M.R. Shoeberl, and E.V. Browell, J. Geophys. Res. D **108**, No. 5, 8312 (2003).
14. S. Hipskind, and S. Gaines, eds., *Airborne Arctic Stratospheric Expedition* (CD-ROM) (NASA Ames Research Center, 1990).
15. S. Gaines, ed., *Airborne Southern Hemisphere Ozone Experiment and Measurements for Assessing the Effects of Stratospheric Aircraft* (CD-ROM) (NASA Ames Research Center, 1995).